analytical chemistry

pubs.acs.org/ac Article

Phosphorus NMR and Its Application to Metabolomics

Fatema Bhinderwala, Paula Evans, Kaleb Jones, Benjamin R. Laws, Thomas G. Smith, Martha Morton, and Robert Powers*

Cite This: *Anal. Chem.* 2020, 92, 9536−9545 Read Online

ACCESS | Metrics & More | Article Recommendations | Supporting Information

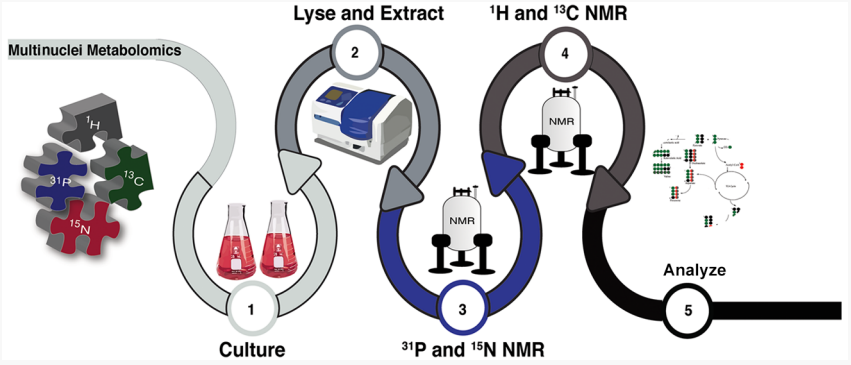

ABSTRACT: Stable isotopes are routinely employed by NMR metabolomics to highlight specific metabolic processes and to monitor pathway flux. ^{13}C-carbon and ^{15}N-nitrogen labeled nutrients are convenient sources of isotope tracers and are commonly added as supplements to a variety of biological systems ranging from cell cultures to animal models. Unlike ^{13}C and ^{15}N, ^{31}P-phosphorus is a naturally abundant and NMR active isotope that does not require an external supplemental source. To date, ^{31}P NMR has seen limited usage in metabolomics because of a lack of reference spectra, difficulties in sample preparation, and an absence of two-dimensional (2D) NMR experiments, but ^{31}P NMR has the potential of expanding the coverage of the metabolome by detecting phosphorus-containing metabolites. Phosphorylated metabolites regulate key cellular processes, serve as a surrogate for intracellular pH conditions, and provide a measure of a cell's metabolic energy and redox state, among other processes. Thus, incorporating ^{31}P NMR into a metabolomics investigation will enable the detection of these key cellular processes. To facilitate the application of ^{31}P NMR in metabolomics, we present a unified protocol that allows for the simultaneous and efficient detection of ^{1}H-, ^{13}C-, ^{15}N-, and ^{31}P-labeled metabolites. The protocol includes the application of a 2D ^{1}H−^{31}P HSQC-TOCSY experiment to detect ^{31}P-labeled metabolites from heterogeneous biological mixtures, methods for sample preparation to detect ^{1}H-, ^{13}C-, ^{15}N-, and ^{31}P-labeled metabolites from a single NMR sample, and a data set of one-dimensional (1D) ^{31}P NMR and 2D ^{1}H−^{31}P HSQC-TOCSY spectra of 38 common phosphorus-containing metabolites to assist in metabolite assignments.

Metabolome profiling techniques have evolved from primitive smell and taste tests to utilizing state-of-the-art analytical instruments.[1] Mass spectrometry (MS) and nuclear magnetic resonance (NMR) spectroscopy are the analytical instrumentation of choice in current metabolomics research.[2] Despite contributing to numerous successes ranging from drug discovery to preventing food adulteration,[3−5] NMR-based metabolomics still faces a number of significant challenges. These include the need for rapid and reliable metabolite annotation, for identifying unknowns, and for increasing the detection of low concentration or transient metabolites. While an NMR metabolomics experiment may detect upward of 100 metabolites, the total human metabolome is estimated to consist of approximately 150,000 metabolites.[6] Thus, for a given cell or biological system the majority of chemical entities comprise the dark metabolome.

Metabolomics relies heavily on the availability of NMR databases that contain various spectral information for known metabolites. Metabolite assignments are thus made by matching the experimental NMR data (*e.g.*, chemical shifts and coupling constants) with reference spectra or data from these databases. A number of NMR databases are available to the metabolomics community.[7−10] While a valuable resource, most NMR databases are heavily populated with 1D ^{1}H and 2D ^{1}H−^{13}C HSQC NMR spectra for commonly available metabolites. There are ongoing efforts to improve database

Received: February 10, 2020
Accepted: June 12, 2020
Published: June 12, 2020

https://dx.doi.org/10.1021/acs.analchem.0c00591
Anal. Chem. 2020, 92, 9536−9545

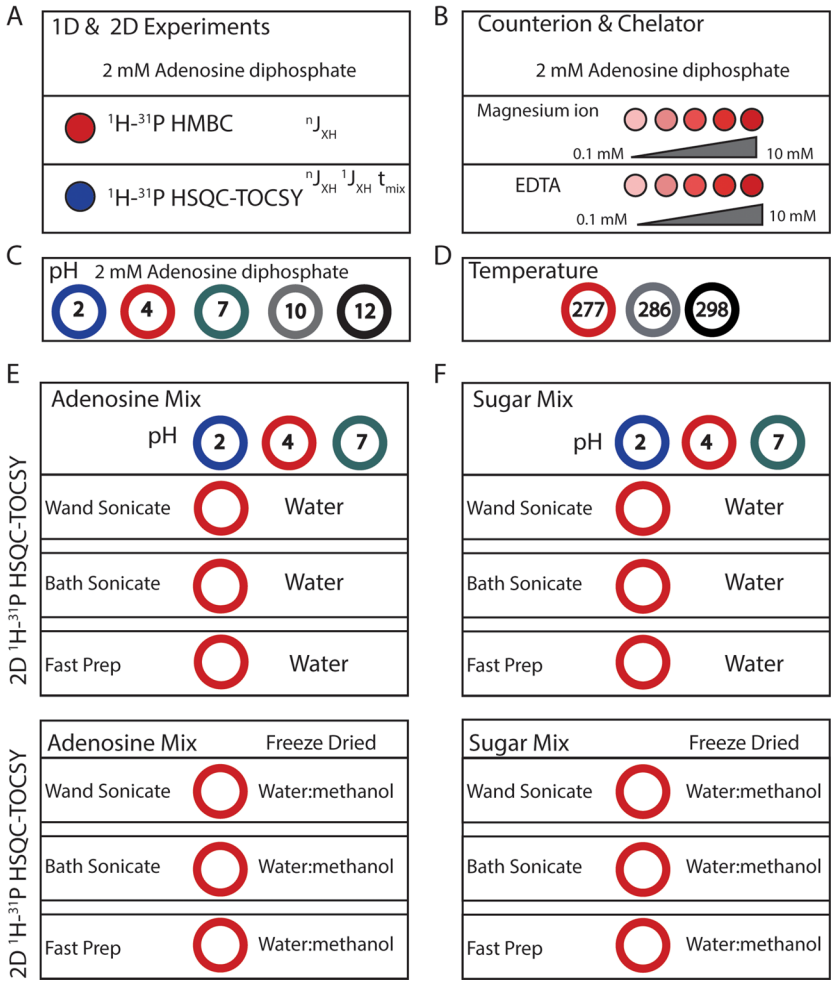

Figure 1. Summary of sample preparations, optimization matrix, and standard samples used to develop a multinuclei metabolomics workflow incorporating ^{31}P NMR. (**A**) Identification of the preferred 2D ^{1}H−^{31}P NMR pulse sequence using a standard 2 mM ADP sample. The one-bond $^{1}J_{X-H}$ coupling constant (160 to 200 Hz), the long-range $^{n}J_{X-H}$ coupling constant (5 to 10 Hz), and the TOCSY mixing time (70 to 120 ms) were optimized. (**B**) The impact of a Mg^{2+} counterion or a chelator (EDTA) on the ADP ^{31}P NMR spectral quality was examined. Similarly, the impact of (**C**) pH and (**D**) temperature on ADP peak width and intensity in both 1D and 2D ^{31}P NMR spectra were evaluated. (**E** and **F**) The stability of phosphorylated metabolites was investigated across a range of experimental conditions using a series of 2D ^{1}H−^{31}P HSQC-TOCSY experiments collected on two different metabolite mixtures (adenosine analogs and sugar phosphates). A range of pH values, extraction solvents, and cell lysing techniques were investigated.

integration, to enhance user tools (*e.g.,* queries), and to expand the spectral content within these databases; however, this has been predominantly directed toward including additional 1D ^{1}H NMR and 2D ^{1}H−^{13}C HSQC spectra for new compounds. This is primarily in response to the routine use of Stable Isotope Resolved Metabolomics (SIRM) experiments, which have nearly exclusively focused on incorporating ^{13}C-carbon labels into the metabolome. Accordingly, various annotation methods have been employed based on ^{1}H−^{1}H or ^{1}H−^{13}C type NMR spectra.[11−14]

Expanding the coverage of the metabolome beyond central carbon metabolism requires alternative SIRM strategies. We and others have recently reported the successful application of ^{15}N NMR to characterize nitrogen-based metabolism in bacterial and mammalian cells by supplementing cell cultures with ^{15}N labeled amino acids.[15,16] Notably, our protocol allowed for the simultaneous detection of both ^{13}C- and ^{15}N-labeled metabolites from a single NMR sample, an effective double-labeled SIRM approach. SIRM methods are an excellent approach for identifying and quantifying metabolites that are not otherwise observed using a 1D ^{1}H NMR untargeted approach.[15] Employing a double-labeled SIRM approach provides a larger coverage of the metabolome, which leads to a better understanding of cellular chemistry or a better approach for identifying biomarkers. While combining ^{13}C- and ^{15}N-based SIRM into a single metabolomics strategy expands the metabolome coverage, why limit the approach to just carbon and nitrogen metabolism? There are other nuclei of biological importance that are NMR active and naturally abundant, such as ^{31}P-phosphorus-containing metabolites. Combining ^{31}P NMR with a multilabeled SIRM approach will only further enhance the metabolome coverage.

^{31}P NMR is an obvious choice to add to an existing multilabeled SIRM approach to metabolomics since ^{31}P is 100% abundant, an NMR active nucleus, and more sensitive than ^{13}C NMR and ^{15}N NMR. More importantly, phosphorus is present in numerous metabolites that regulate major cellular processes. In fact, phosphorylated metabolites may comprise upward of 36% of the known metabolome (based on the percentage of phosphorylated metabolites in HMDB).[7] NMR

https://dx.doi.org/10.1021/acs.analchem.0c00591
Anal. Chem. 2020, 92, 9536−9545

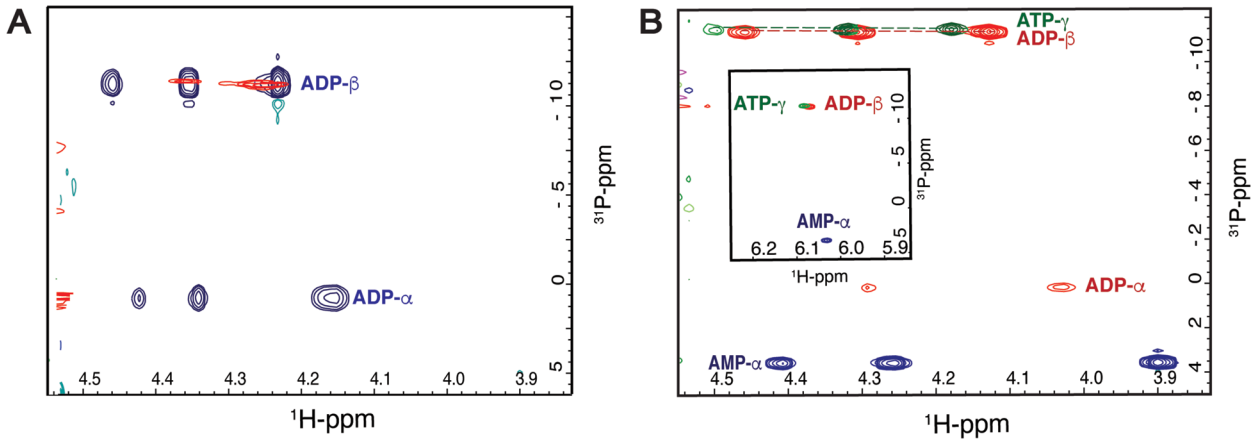

Figure 2. Representative examples of 2D ^{1}H−^{31}P NMR spectra. (**A**) Overlay of 2D ^{1}H−^{31}P HSQC-TOCSY (blue) and 2D ^{1}H−^{31}P HMBC (red) spectra acquired for a 1 mM solution of adenosine diphosphate (ADP) in a 90:10 water:D_2O solution at pH 4. (**B**) Overlay of 2D ^{1}H−^{31}P HSQC-TOCSY spectra with an 80 ms TOCSY mixing time for a 2 mM solution of adenosine monophosphate (AMP) (blue), adenosine diphosphate (ADP) (red), and ATP (green) in a 90:10 water:D_2O solution at pH 4.

is also uniquely capable of simplifying spectral information by using nuclei-specific filtering, which provides an elegant and robust way to only observe phosphorylated metabolites.

1D ^{31}P NMR was extensively used in the early application of NMR to study cellular biochemistry,[17] to investigate various diseases,[18,19] as a tool of synthetic chemistry,[20] and to explore DNA and RNA structures;[21−23] but ^{31}P NMR methods have seen limited use of late and have not been systematically assessed for metabolomics application, and a robust workflow has not been developed to facilitate a wider adoption by the metabolomics community. There are a number of known challenges to the application of ^{31}P NMR to metabolomics, such as a lack of chemical shift references, the large pH and temperature dependence of the chemical shifts, and the poor line shapes that are further complicated by various phosphorus ionization states and the diversity of bound ions. There has also been the perception that at higher magnetic field strengths chemical shift anisotropy would render the ^{31}P spectrum useless with no baseline resolution of peaks. However, by addressing these concerns, ^{31}P NMR may serve the NMR-metabolomics community and shed some light on the dark metabolome.

Herein, we systematically explored the potential for ^{31}P-based NMR metabolomics. 1D ^{31}P and various different 2D pulse sequences were evaluated, and an optimized 2D ^{1}H−^{31}P HSQC-TOCSY spectrum is proposed as the preferred choice to identify phosphorus-containing metabolites. A set of 1D ^{31}P and 2D ^{1}H−^{31}P HSQC-TOCSY spectra for 38 common phosphorus compounds has been acquired to aid in the annotation of phosphorus-containing metabolites. Importantly, an overall protocol for a multinuclei approach to metabolomics is presented that provides an efficient integration of ^{31}P NMR with multi-SIRM for the simultaneous detection of ^{1}H-, ^{13}C-, ^{15}N-, and ^{31}P-containing metabolites from a single NMR sample. In total, the multinuclei metabolomics protocols and reference spectra are expected to enable the metabolomics community to adopt ^{31}P NMR for characterizing biological samples and expanding the coverage of the metabolome.

METHODS

Study Design. An overview of the series of experiments used to optimize and implement a ^{31}P NMR protocol into a multinuclei metabolomics workflow is diagramed in Figure 1. As described in detail in the Supporting Information, a series of standard metabolite and metabolite mixture samples (Tables S1 and S2) were used to optimize experimental parameters, sample conditions, and metabolome extraction protocols and to identify the preferred ^{31}P NMR pulse sequence. Specifically, a range of pH values (2, 4, 7, 10, and 12), temperatures (277, 286, and 298 K), Mg^{2+} concentrations (0.1 to 10 mM), and EDTA concentrations (0.1 to 10 mM) were investigated to optimize sample conditions in order to maximize spectral quality and sample stability. Similarly, different extraction solvents (100% water, 1:1 water:methanol, and 1:1 methanol:-chloroform), cell lysing techniques (wand sonicator, water-bath sonicator, and FastPrep bead beating), and sample drying (SpedVac and lyophilizer) were investigated to maximize the presence of phosphorylated-metabolites in a metabolomics sample. 1D ^{31}P, 2D ^{1}H−^{31}P HSQC-TOCSY, and 2D ^{1}H−^{31}P HMBC pulse sequences were explored to identify the preferred ^{31}P NMR pulse sequence. Also, the one-bond $^{1}J_{X-H}$ coupling constant (160 to 200 Hz), the long-range $^{n}J_{X-H}$ coupling constant (5 to 10 Hz), and the TOCSY mixing time (70 to 120 ms) were optimized to maximize spectral quality and the number of detectable NMR resonances. See the Supporting Information for further details on the routine protocols used for NMR data collection, processing, and metabolite assignments and for the list of chemicals used in this study.

RESULTS AND DISCUSSION

Optimization of NMR Experimental Parameters. Phosphorus chemical shifts and line shapes are significantly influenced by solvent, pH, counterion, ionic strength, and temperature. ^{31}P resonances have a limited chemical shift dispersion and tend to be broad, leading to obscured peak splitting. Furthermore, phosphorus-containing metabolites are of relatively low stability. Consequently, ^{31}P NMR has seen limited application in recent metabolomics studies despite being a 100% abundant nuclei with relatively high sensitivity. Instead, NMR researchers tend to utilize the incorporation of expensive ^{13}C and ^{15}N isotope labeling to characterize the metabolome. Alternatively, natural abundant ^{13}C NMR is also routinely employed for the analysis of biofluids but at the expense of longer NMR acquisition time.[24,25] Of course, either

https://dx.doi.org/10.1021/acs.analchem.0c00591
Anal. Chem. 2020, 92, 9536−9545

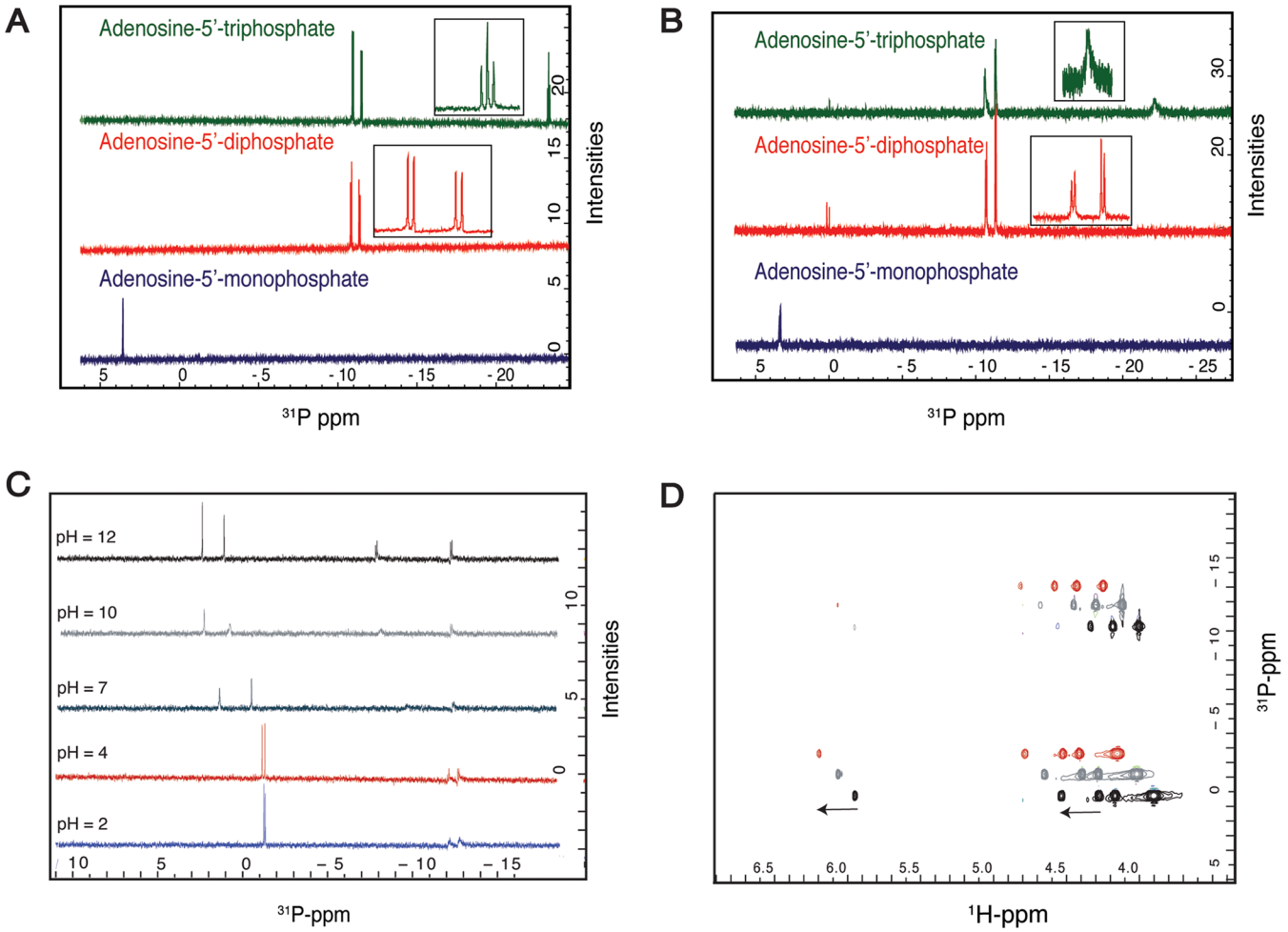

Figure 3. Impact of pH and temperature on 1D and 2D ^{31}P NMR spectra. Stacked plots of 1D ^{31}P spectra for a 2 mM solution of AMP (blue), ADP (red), and ATP (green) in a 90:10 water:D_2O solution at pH 4 (**A**) without and (**B**) with the addition of 2 mM Mg^{2+}. (**C**) Stacked plots of 1D ^{31}P spectra for a 2 mM solution of ADP in a 90:10 water:D_2O solution at pH values of 2, 4, 7, 10, and 12. (**D**) Overlay of 2D ^{1}H−^{31}P HSQC-TOCSY spectra of a 1 mM solution of ADP in a 90:10 water:D_2O solution at three different temperatures corresponding to 298 K (black), 286 K (gray), and 277 K (red).

approach may limit the coverage of the metabolome while providing an incomplete view of system perturbations. To address some of the inherent challenges with ^{31}P NMR and to increase its broad application, a variety of experimental conditions were investigated to develop a routine and robust ^{31}P NMR metabolomics approach. An ideal NMR metabolomics experiment has four defining characteristics: (i) sharp, resolved, and quantifiable peaks, (ii) highly stable and reproducible data, (iii) high-throughput and rapid data acquisition, and (iv) sufficient spectral information to readily identify the compounds. In this regards, 2D ^{1}H−^{31}P pulse sequences were systematically evaluated to identify an ideal experiment for the identification and quantification of phosphorus-containing metabolites.

The 2D ^{1}H−^{31}P HSQC-TOCSY and ^{1}H−^{31}P HMBC pulse sequences were first evaluated using adenosine diphosphate (ADP). An overlay of the two ADP spectra is shown in Figure 2A. The spectral overlay clearly highlights the significant increase in spectral information in the 2D ^{1}H−^{31}P HSQC-TOCSY spectrum relative to the HMBC spectrum. A greater number of ^{1}H−^{31}P correlations were observed in the HSQC-TOCSY spectrum, which are critical for an accurate identification of phosphorus-containing metabolites. Simply, the limited ^{31}P chemical shift dispersion makes it difficult to make an unambiguous metabolite assignment based strictly on ^{31}P chemical shifts. This occurs because most phosphorus-containing compounds are structurally similar to other metabolites. For example, the phosphate group within both adenosine monophosphate (AMP) and cytidine monophosphate (CMP) is attached to the same sugar moiety. Thus, accurate metabolite assignments require correlated ^{1}H chemical shifts. Accordingly, we focused our further efforts on optimizing the 2D ^{1}H−^{31}P HSQC-TOCSY experimental parameters to maximize its utility in a metabolomics study. Notably, Gradwell et al. supported our conclusion, where the 2D ^{1}H−^{31}P HSQC-TOCSY experiment was successfully used to identify metabolites from a complex mixture derived from crayfish.[18]

A series of 2D ^{1}H−^{31}P HSQC-TOCSY spectra were collected using the ADP sample while varying the one-bond $^{1}J_{X-H}$ coupling constant, the long-range $^{n}J_{X-H}$ coupling constant, and the TOCSY mixing time. Specifically, the $^{1}J_{X-H}$ values were varied between 160 and 200 Hz (20 Hz increments), the $^{n}J_{X-H}$ values were varied between 5 and 10 Hz (1 Hz increment), and the mixing time was varied between 70 and 120 ms (10 ms increment). All other experimental

https://dx.doi.org/10.1021/acs.analchem.0c00591
Anal. Chem. 2020, 92, 9536−9545

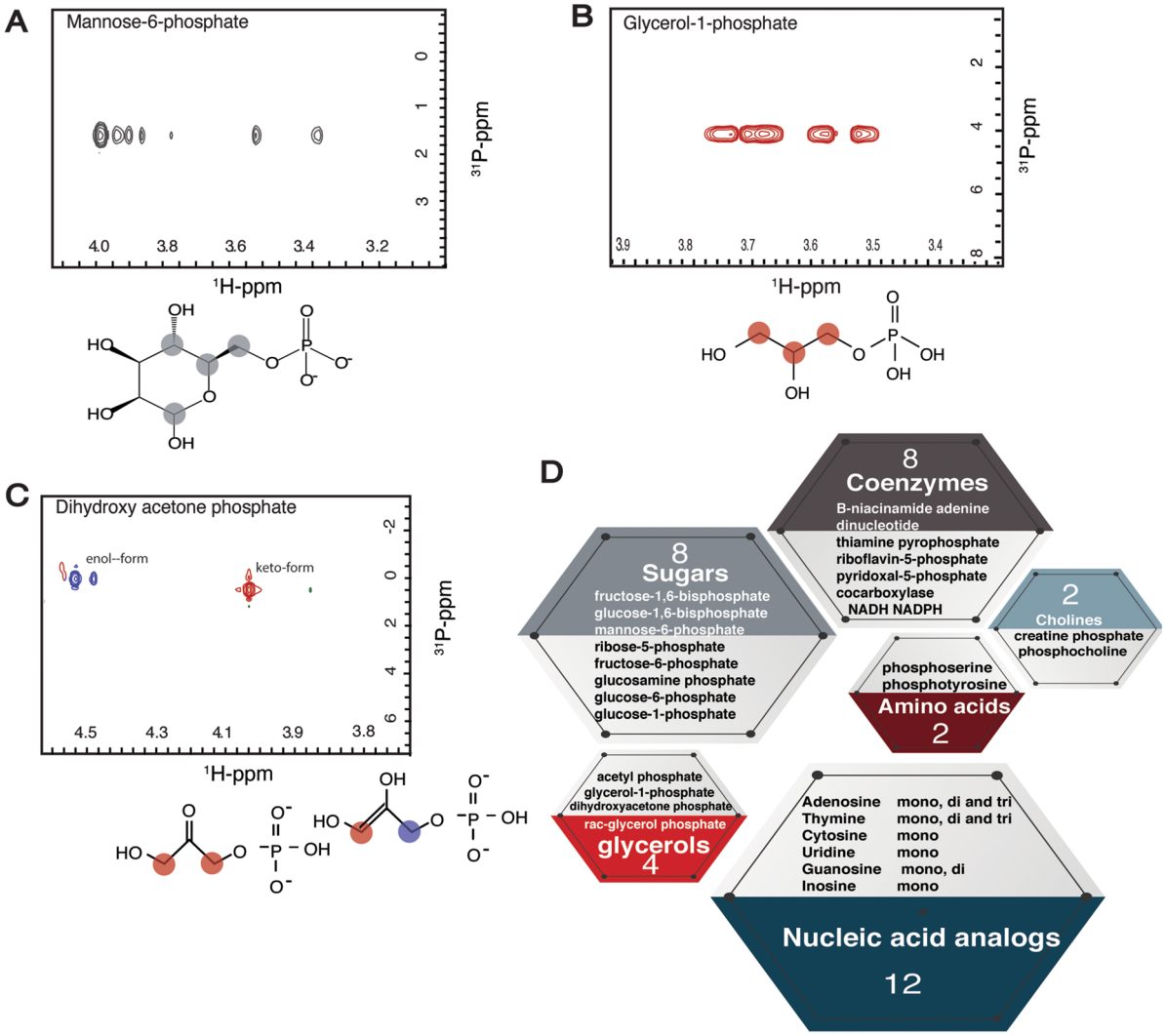

Figure 4. Representative 2D ^{1}H -^{31}P HSQC-TOCSY spectra using a 80 ms mixing time for (**A**) mannose-6-phosphate, (**B**) glycerol-1-phosphate, and (**C**) dihydroxy acetone phosphate (enol (blue) and keto (red) forms are labeled). The chemical structures are shown under each spectrum where each observed correlation is indicated by a circle. (**D**) Summary of the 38 phosphorylated compounds and their assigned chemical class for which 1D ^{31}P and 2D ^{1}H -^{31}P HSQC-TOCSY spectra were acquired.

parameters remained constant. The resulting spectral data set was qualitatively evaluated based on the number of observed ^{1}H-correlations and the overall spectral signal-to-noise. Notably, the choice of TOCSY mixing time had the greatest impact on spectral quality (Figure 2B). The optimal 2D ^{1}H−^{31}P HSQC-TOCSY experiment used a one-bond $^{1}J_{X-H}$ coupling constant of 200 Hz, a long-range $^{n}J_{X-H}$ coupling constant of 8 Hz, and a TOCSY mixing time of 80 ms. A similar effort to optimize the 2D ^{1}H−^{31}P HMBC experiment yielded no improvement to the spectrum shown in Figure 2A.

Optimization of Sample Preparation Parameters. ^{31}P chemical shifts may be sensitive to the type and charge of counterions present in the sample buffer. For example, magnesium ion (Mg^{2+}) is traditionally used in DNA structural analysis to aid in ^{31}P chemical shift dispersion.[19,26−28] Thus, the impact of double charged counterion species on common phosphorus-containing metabolites was evaluated. Specifically, AMP, ADP, and ATP NMR samples were titrated with upwards of 10 mM of $MgCl_2$ or EDTA. The ^{31}P chemical shift variation was monitored as a function of each titrant. Only a minimal impact on the β and α phosphate signal was observed in the 1D ^{31}P spectrum (Figure 3**A, B**). Similarly, the chemical shifts in the 2D ^{1}H−^{31}P HSQC-TOCSY spectrum (Figure 3**A**) were essentially unaffected by the addition of Mg^{2+}. While the addition of Mg^{2+} had a minimal impact on ^{31}P chemical shifts, it did affect peak shape and line widths. The effect of Mg^{2+} on ^{31}P line shape may be explained by a change in the P−OH bond angle.[29] A bound Mg^{2+} likely restricts the free movement of the outermost phosphate, which leads to a rigid structure and sharp lines. Thus, the addition of Mg^{2+} improves the overall quality of the ^{31}P spectrum by decreasing line width while minimally impacting chemical shifts. Accordingly, an optimal ^{31}P spectrum is achieved by adding 2 mM of Mg^{2+} to each metabolomics sample, but the addition of Mg^{2+} is not essential.

As previously demonstrated with our combined ^{13}C and ^{15}N SIRM protocol,[30] the proper choice of pH and temperature is integral to streamlining a multinuclei metabolomics workflow. Accordingly, the effect of pH and temperature on ^{31}P chemical shifts and peak intensities was thoroughly investigated. A stacked plot of 1D ^{31}P spectra for ADP at pH values ranging from 2 to 12 is shown in Figure 3C. The impact of pH on the

https://dx.doi.org/10.1021/acs.analchem.0c00591
Anal. Chem. 2020, 92, 9536−9545

quality of the ^{31}P spectrum was quite dramatic and is likely attributed to changes in both the stability and ionization state of the phosphate group. This is consistent with previous reports that the stability of ATP is increased at either acidic or basic pH values.[31,32] Accordingly, a pH of 4 was determined to be optimal for collecting a ^{31}P spectrum of metabolomics samples. Importantly, a low pH is also compatible with the sample conditions we previously reported for detecting nitrogen-containing metabolites.

An overlay of the 2D ^{1}H−^{31}P HSQC-TOCSY spectra for ADP at three different temperatures (277, 286, and 298 K) is shown in Figure 3D. Not surprisingly, temperature also impacted the quality of the NMR spectrum for phosphorus-containing metabolites. In addition to the expected uniform downfield temperature-dependent shift, an increase in temperature also resulted in a broadening of peaks and a loss in some observable ^{1}H-correlations. Accordingly, the best-quality 2D ^{1}H−^{31}P HSQC-TOCSY spectrum was obtained at 277 K. Two mixtures comprised of different sets of phosphorus-containing metabolites (*e.g.,* sugar phosphates and adenosine analogs) were used to further verify (*data not shown*) that a sample pH of 4 and a temperature of 277 K yielded the best results. To summarize, a 2D ^{1}H−^{31}P HSQC-TOCSY spectrum at 277 K of a metabolomics sample prepared in 10% D_2O/90% H_2O titrated to a pH of 4 provides the best approach to properly characterize phosphorus-containing metabolites. Note, a standard phosphate buffer is not recommended because of dynamic range problems with low abundant metabolites. Furthermore, the addition of other buffers is also not preferred since it may require a buffer exchange and extensive sample handling to collect subsequent ^{1}H, ^{13}C, and ^{15}N spectra from the same metabolomics sample. Since ^{31}P chemical shifts are very pH sensitive, care is required to minimize any pH variance between NMR metabolomics samples. This is achievable by either using an internal pH standard or by manually verifying each sample's pH value, which is our preferred method.

Database of 1D ^{31}P and 2D ^{1}H−^{31}P HSQC-TOCSY Spectra for Common Metabolites. A set of 1D ^{31}P and 2D ^{1}H−^{31}P HSQC-TOCSY spectra was acquired for 38 readily accessible phosphorus-containing compounds (Table S1) utilizing the optimized experimental parameters described above. The set of 38 metabolites consists of a wide variety of chemically distinct phosphate compounds that are primarily monophosphates. The metabolites can be grouped into six general classes comprising amino acids, cholines, and others, coenzymes, glycerols, nucleic acid analogs, and sugars (Figure 4**A, C**). A good quality NMR spectrum was acquired for all compounds at a concentration of 2 mM. The 1D ^{31}P and 2D ^{1}H−^{31}P HSQC-TOCSY spectra required a total acquisition time of approximately 1 h. The 2D ^{1}H−^{31}P HSQC-TOCSY experiment was collected using nonuniform sampling at a 25% sparsity with our deterministic sampling scheme.[33] A few representative 2D ^{1}H−^{31}P HSQC-TOCSY spectra are shown in Figure 3**B−D,** which correspond to dihydroxy acetone phosphate (both keto and enol resonance forms are present),[34] glycerol-1-phosphate, and mannose-6-phosphate. Notably, dihydroxy acetone phosphate and glycerol-1-phosphate are glycolytic intermediates, which are crucial regulatory steps and connect to other principle pathways. While the compounds have similar structures, a distinct peak pattern is observed in the 2D ^{1}H−^{31}P HSQC-TOCSY spectrum enabling easy metabolite assignments. The chemical shifts from the 1D ^{31}P and 2D ^{1}H−^{31}P HSQC-TOCSY spectra are summarized in Tables S1 and S2. Two different sets of spectral data are provided, one corresponding to the pH that simply results from dissolving the metabolites in water and another where all the metabolites were adjusted to a final pH of 4. Unsurprisingly, phosphorus-containing compounds induce a wide range of pH values (2.3 to 7.7) in an unbuffered solution. The database of ^{31}P NMR spectra provides a means to readily assign metabolites detected in cell lysates or other biological samples. Phosphorylated metabolites are often hard to distinguish using routine ^{1}H and ^{13}C spectral data. To further facilitate the assignment of phosphorylated metabolites, 2D ^{1}H−^{13}C HSQC spectra of the 38 phosphorylated metabolites were also collected at pH 4. The pH 4 ^{1}H and ^{13}C chemicals shifts are listed in Table S3.

Stability of Phosphorus-Containing Metabolites and the Impact of Extraction Protocols. Phosphorylated metabolites are prone to hydrolysis, which leads to the accumulation of inorganic phosphate and its related substrate.[31,35] The rate and extent of chemical hydrolysis is influenced by pH, temperature, and the presence of counterions.[32] Phosphorylated metabolites are also prone to enzymatic hydrolysis.[32] For example, in a cell lysate, the presence of active phosphatases may hasten the hydrolysis of labile phosphate groups, which may result in the loss of multiply phosphorylated species. Thus, sample handling and metabolome extraction processes may induce biologically irrelevant changes to the metabolome and lead to erroneous interpretations. To address these issues, the impact of common extraction processes on the stability of phosphorus-containing metabolites was evaluated with two different metabolite mixtures. One mixture consisted of adenosine nucleotide analogs, and the second mixture contained sugar phosphates (Table S4).

Three common metabolite extraction processes were evaluated to identify an optimal sample preparation protocol for ^{31}P NMR. The experimental design and extraction protocols are summarized in Figure 1. Each metabolite extraction protocol is comprised of three primary components: (i) an extraction solvent, (ii) a cell lysing method, and (iii) a sample drying method. Accordingly, the adenosine analogs and sugar phosphate mixtures were treated with pure water or a 1:1 water:methanol extraction solvent. The samples were then either sonicated with a wand or water bath or subjected to bead beating in Lysing matrix B using a FastPrep. The water:methanol samples were then dried using a combination of a SpeedVac evaporator and a lyophilizer. In total, 14 NMR samples were prepared, seven for each of the adenosine analogs and sugar phosphate mixtures. The final NMR samples consisted of a 10% D_2O/90% H_2O solvent manually adjusted to a pH of 4. A 1D ^{31}P spectrum and a 2D ^{1}H−^{31}P HSQC TOCSY spectrum were acquired for each sample. Representative 2D ^{1}H−^{31}P HSQC TOCSY spectra of the adenosine analog and sugar phosphate mixtures are shown in Figures S1 and S2, respectively.

As evident by the spectral overlays in Figure S1A, B, there were no detectable changes in the NMR spectra after sonication or sample drying. However, significant sample degradation was observed after subjecting the samples to a FastPrep bead beating (Figure S1C). Sample heating during the bead beating process along with the presence of the silica-based beads may have negatively impacted the stability of the adenosine analogs. The combination of sample drying and FastPrep bead beating also decreased the stability of the sugar

https://dx.doi.org/10.1021/acs.analchem.0c00591
Anal. Chem. 2020, 92, 9536−9545

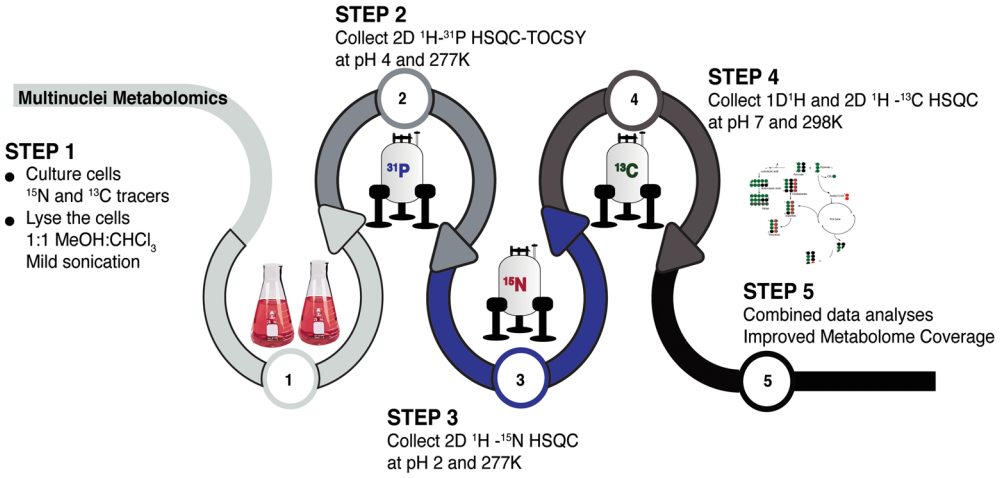

Figure 5. Summary of the multinuclei NMR metabolomics workflow. ^{1}H-, ^{13}C-, ^{15}N-, and ^{31}P-metabolites are characterized from a single sample by collecting a sequential series of 2D NMR experiments corresponding to a 2D ^{1}H−^{31}P HSQC-TOCSY, 2D ^{1}H−^{15}N HSQC, and 2D ^{1}H−^{13}C HSQC. The order of the experiments is intended to preserve the labile metabolites.

phosphate mixture (Figure S2C). Notably, the decrease in the sugar phosphate mixture was not as pronounced as observed for the adenosine analog mixture. These results illustrate the importance of employing a mild metabolome extraction method to ensure maximum recovery of phosphorylated metabolites.

A Multinuclei (^{1}H, ^{13}C, ^{15}N, and ^{31}P) Metabolomics Workflow. Two bacterial cell lysates and a yeast cell lysate were used to demonstrate a multinuclei metabolomics workflow. Specifically, ^{1}H, ^{13}C, ^{15}N, and ^{31}P NMR data are sequentially obtained from a single, multi-isotope labeled cell lysate. The overall multinuclei metabolomics protocol is summarized in Figure 5. Briefly, cells are cultured in a medium supplemented with both a ^{13}C-labeled and a ^{15}N-labeled nutrient. The metabolome is then extracted with a cold 1:1 methanol:chloroform solvent followed by mild sonication while keeping the sample on ice. The metabolomics sample is dried using a combined SpeedVac and lyophilizer and then reconstituted with 10% D_2O/90% H_2O that is manually titrated to a pH of 4. The ^{31}P NMR spectrum is collected first because of the inherently lower stability of phosphorylated metabolites. It also solves the buffer problem. Most NMR metabolomics experiments are done with samples containing a millimolar concentration of a phosphate buffer. Such a high concentration of inorganic phosphate would be expected to mask any phosphorus-containing metabolites in the sample due to limitations in dynamic range. A 1D ^{31}P spectrum and a 2D ^{1}H−^{31}P HSQC TOCSY spectrum are collected at 277 K. The metabolomics sample is then adjusted to a pH of 2 by either the addition of DCl or an appropriate aliquot of a 1 M stock solution of a phosphate buffer at pH 2. The final metabolomics sample contains 25 mM of a phosphate buffer and 500 μM of TMSP. A 2D ^{1}H−^{15}N HSQC spectrum is collected at 277 K. The sample is then titrated up to pH 7 with NaOD, and a 1D ^{1}H spectrum and a 2D ^{1}H−^{13}C HSQC spectrum are collected at 298 K.

E. coli cells were grown in M9 minimal media supplemented with uniformly ^{13}C-labeled glucose and $^{15}NH_3Cl$ as the sole carbon and nitrogen sources, respectively. Similarly, the sodium phosphate salts in the culture medium serve as the sole phosphate source for the bacteria. *E. coli* simply incorporates the ^{13}C-carbon, the ^{15}N-nitrogen, and the phosphate into various cellular metabolites. An initial 2D ^{1}H−^{31}P HSQC TOCSY spectrum (*data not shown*) exhibited a very limited number of chemical shifts that were assigned to only a few monophosphorylated metabolites. This observation suggested that the extraction method may have resulted in the degradation of labile phosphorylated metabolites. The extraction process was subsequently modified by replacing the 1:1 water:methanol solvent with a 1:1 methanol:chloroform mixture. The resulting 2D ^{1}H−^{31}P HSQC TOCSY spectrum had a notable increase in the number peaks, and five different phosphorylated metabolites were assigned. Representative 2D ^{1}H−^{31}P HSQC TOCSY, ^{1}H−^{15}N HSQC, and ^{1}H−^{13}C HSQC spectra obtained from the *E. coli* cell lysate are shown in Figure 6. In this manner, the entire detectable ^{1}H-, ^{13}C-, ^{15}N-, and ^{31}P-containing metabolome is completely characterized from a single sample using three different 2D NMR spectra. Although the entire multinuclei metabolomics process requires additional sample handling and multiple pH changes, a comparison of the 2D ^{1}H−^{13}C HSQC spectrum from the multinuclei metabolomics data set to spectra acquired following the traditional ^{13}C labeling method resulted in no detectable variation in the number of peaks or in peak intensities (Figure S3). This observation suggests the composition of a metabonomics sample is relatively stable to wide changes in pH, which is consistent with prior reports.[36,37] Furthermore, the acquisition of a 1D ^{1}H spectrum at pH 7 as part of the multinuclei metabolomics protocol permits for straightforward assignment of metabolites using the abundance of database information that is only available at pH 7. A 2D ^{1}H−^{31}P HSQC TOCSY spectrum was also acquired for *M. smegmatis* and *S. pombe* (Figure S4). However, efficient lysing of these cells required a harsher FastPrep bead beating method.[38] Consequently, fewer metabolite peaks were observed in the ^{31}P NMR spectra, which could not be assigned to any common metabolite. Clearly, the application of ^{31}P NMR to accurately characterize phosphorus-containing metabolites is restricted to mild types of cell lysing and extraction techniques. Overall, the multinuclei metabolomics protocol is a versatile approach for interrogating metabolomes from a variety of biological sources by using any combination of traditional isotope-labeling schemes and naturally abundant nuclei. In this regard, our multinuclei metabolomics protocol

https://dx.doi.org/10.1021/acs.analchem.0c00591
Anal. Chem. 2020, 92, 9536−9545

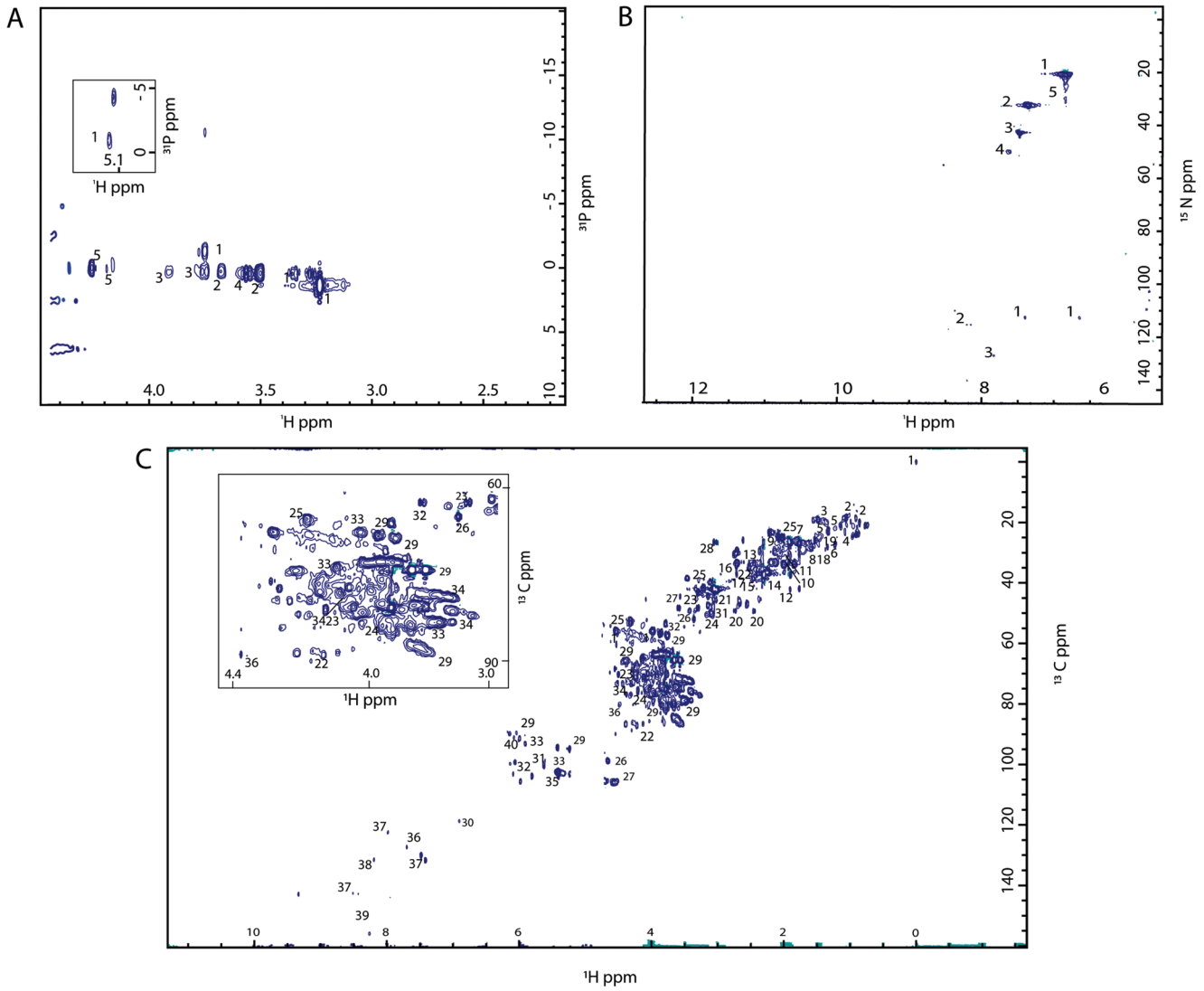

Figure 6. (**A**) 2D ^{1}H−^{31}P HSQC-TOCSY, (**B**) 2D ^{1}H−^{15}N HSQC, and (**C**) 2D ^{1}H−^{13}C HSQC spectra collected from *E. coli* grown in M9 minimal media supplemented with $^{15}NH_3Cl$ and $^{13}C_6$ glucose. Cells were harvested during the log phase. The metabolite assignments correspond to the following: 1: glucose-1,6-biphosphate, 2: glucose-6-phosphate, 3: ribose-5-phosphate, 4: AMP, and 5: glycerol phosphate in (**A**); 1: arginine, 2: glutamine, 3: asparagine, 4: 5-azacytidine, and 5: glutamate in (**B**); 1: TMSP, 2: valine, 3: alanine, 4: *N*-acetyl alanine, 5: leucine, 6: beta-leucine, 7: lactate, 8: 2-hydroxy-3-methyl butyrate, 9: acetyl carnithine, 10: *N*-acetyl aspartate, 11: *N*-acetyl glucosamine, 12: ornithine, 13: aminobutyrate, 14: acetate, 15: arginine, 16: *N*-acetyl ornithine, 17: cystathionine, 18: aminohexanoic acid, 19: 2-hydroxy butyrate, 20: malate, 21: pyruvate, 22: lysine, 23: glutamate, 24: glutamine, 25: *N*-acetyl glutamate, 26: succinate, 27: citrulline, 28: coenzyme A, 29: glucose, 30: fumarate, 31: proline, 32: isoleucine, 33: fructose, 34: glycerol, 35: phosphoenolpyruvate, 36: UDP-glucose, 37: AMP, 38: NAD, and 39: glucose-6-phosphate in (**C**).

can obtain a comprehensive characterization of the entire metabolome.

CONCLUSIONS

^{31}P NMR offers significant benefits to the metabolomics field by expanding the coverage of the metabolome and by enabling the detection of metabolites integral to critical cellular processes, such as energy metabolism and cell signaling. Metabolite assignments may be further validated or confirmed by combining the analysis from multiple NMR spectra. For example, a phosphorus-containing metabolite may be inferred from a 2D ^{1}H−^{13}C HSQC spectrum but may be directly detected and validated from the 2D ^{1}H−^{31}P HSQC-TOCSY spectrum. Similarly, ^{13}C/^{15}N-SIRM experiments only detect and quantify the amount of the metabolite that is directly derived from the ^{13}C or ^{15}N source. Conversely, the 2D ^{1}H−^{31}P HSQC-TOCSY spectrum will yield the total metabolite concentration. Thus, differences in relative metabolite concentrations from the 2D ^{1}H−^{13}C/^{15}N HSQC and ^{1}H−^{31}P HSQC-TOCSY spectra may provide insights regarding variable nitrogen, carbon, and phosphorus flux through different metabolic processes. To capitalize on these advantages, we have described a standard multinuclei metabolomics workflow that incorporates ^{31}P NMR into a metabolomics strategy. Our multinuclei metabolomics protocol enables the characterization of the entire detectable ^{1}H-, ^{13}C-, ^{15}N-, and ^{31}P-containing metabolome using a single sample and a series of 2D NMR spectra. Again, the availability of different types of 2D NMR spectra will also improve the reliability and accuracy of metabolite assignments. A standard protocol for collecting 2D ^{1}H−^{31}P HSQC-TOCSY spectra as part of a multinuclei metabolomics workflow was presented.

https://dx.doi.org/10.1021/acs.analchem.0c00591
Anal. Chem. 2020, 92, 9536−9545

The coupling constants and TOCSY mixing times for the 2D $^{1}H-^{31}P$ HSQC-TOCSY pulse sequence were optimized to maximize the detection and annotation of phosphorylated-metabolites. Similarly, sample conditions and metabolome extraction protocols were investigated to enable the sequential detection of ^{1}H, ^{13}C, ^{15}N, and ^{31}P NMR spectra while minimizing sample handling and preserving phosphorylated metabolites. Accordingly, the ^{31}P NMR spectra needs to be acquired first. The sample needs to be at a pH of 4 and a temperature of 277 K, and a standard phosphate buffer is only added after the ^{31}P NMR spectra are collected. To facilitate the ready assignment of phosphorus-containing metabolites, a reference library of 1D ^{31}P and 2D $^{1}H-^{31}P$ HSQC-TOCSY spectra with associated chemical shift assignments was assembled for 38 common phosphorylated-metabolites.

^{31}P NMR avoids the expensive isotope labeling costs encountered with ^{13}C- and ^{15}N-SIRM and requires minimal instrument time due to its higher intrinsic sensitivity. This is particularly valuable for studies involving animal models or human clinical samples where isotope labeling may be prohibitive. Of course, natural abundant ^{13}C NMR has been routinely and successfully employed to characterize various clinical metabolomics samples (*e.g.*, urine and serum) or cell extracts.[24,25] Despite the advantages of ^{31}P NMR, there are also notable challenges. Minimal ^{31}P chemical shift dispersion requires 2D NMR experiments for reliable metabolite identification. ^{31}P NMR is also hindered by the low stability of phosphorylated metabolites, which are readily hydrolyzed and may give a false view of the true biological distribution. Thus, great care is required to preserve phosphorylated metabolites that includes a low temperature, a methanol:-chloroform extraction solvent, and mild cell lysing techniques. Despite these challenges, ^{31}P NMR should be a routine component of a metabolomics study since it can provide valuable information and novel insights that are not achievable by other techniques.

■ ASSOCIATED CONTENT

Supporting Information

The Supporting Information is available free of charge at https://pubs.acs.org/doi/10.1021/acs.analchem.0c00591.

Materials and methods related to NMR sample preparation, NMR data acquisition for optimal sample conditions, standard phosphorylated metabolites, and metabolite assignments, figures showing impact of sample preparation protocols and metabolomics test cases for *S. pombe* and *M. smegmatis*, and tables with list of chemical shifts for phosphorylated metabolites at pH 4, their native pH, and composition of mixtures used in study (PDF)

■ AUTHOR INFORMATION

Corresponding Author

Robert Powers − *Department of Chemistry and Nebraska Center for Integrated Biomolecular Communication, University of Nebraska-Lincoln, Lincoln, Nebraska 68588-0304, United States;* orcid.org/0000-0001-9948-6837; Phone: (402) 472-3039; Email: rpowers3@unl.edu; Fax: (402) 472-9402

Authors

Fatema Bhinderwala − *Department of Chemistry and Nebraska Center for Integrated Biomolecular Communication, University of Nebraska-Lincoln, Lincoln, Nebraska 68588-0304, United States*

Paula Evans − *Department of Chemistry, University of Nebraska-Lincoln, Lincoln, Nebraska 68588-0304, United States*

Kaleb Jones − *Department of Chemistry, University of Nebraska-Lincoln, Lincoln, Nebraska 68588-0304, United States*

Benjamin R. Laws − *Department of Chemistry, University of Nebraska-Lincoln, Lincoln, Nebraska 68588-0304, United States*

Thomas G. Smith − *Department of Chemistry and Nebraska Center for Integrated Biomolecular Communication, University of Nebraska-Lincoln, Lincoln, Nebraska 68588-0304, United States*

Martha Morton − *Department of Chemistry and Nebraska Center for Integrated Biomolecular Communication, University of Nebraska-Lincoln, Lincoln, Nebraska 68588-0304, United States;* orcid.org/0000-0002-6411-1733

Complete contact information is available at: https://pubs.acs.org/10.1021/acs.analchem.0c00591

Author Contributions

F.B., P.E., B.R.L., T.G.S., and K.J. performed the experiments; F.B., M.M., and R.P. designed the experiments; F.B., M.M., and R.P. analyzed the data and wrote the manuscript.

Notes

Any opinions, findings, and conclusions or recommendations expressed in this material are those of the author(s) and do not necessarily reflect the views of the National Science Foundation.

The authors declare no competing financial interest.

■ ACKNOWLEDGMENTS

This material is based upon work supported by the National Science Foundation under Grant Number 1660921. This work was supported in part by funding from the Redox Biology Center (P30 GM103335, NIGMS) and the Nebraska Center for Integrated Biomolecular Communication (P20 GM113126, NIGMS). The research was performed in facilities renovated with support from the National Institutes of Health (RR015468-01).

■ REFERENCES

(1) Gebregiworgis, T.; Powers, R. *Comb. Chem. High Throughput Screening* **2012**, *15* (8), 595−610.

(2) Marshall, D. D.; Powers, R. *Prog. Nucl. Magn. Reson. Spectrosc.* **2017**, *100*, 1−16.

(3) Bhinderwala, F.; Powers, R. NMR Metabolomics Protocols for Drug Discovery. In *NMR-Based Metabolomics: Methods and Protocols*; Gowda, G. A. N., Raftery, D., Eds.; Springer New York: New York, NY, 2019; pp 265−311, DOI: 10.1007/978-1-4939-9690-2_16.

(4) Jung, Y.; Lee, J.; Kwon, J.; Lee, K.-S.; Ryu, D. H.; Hwang, G.-S. *J. Agric. Food Chem.* **2010**, *58* (19), 10458−10466.

(5) Amargianitaki, M.; Spyros, A. *Chem. Biol. Technol.* **2017**, *4* (1), 9.

(6) Markley, J. L.; Brüschweiler, R.; Edison, A. S.; Eghbalnia, H. R.; Powers, R.; Raftery, D.; Wishart, D. S. *Curr. Opin. Biotechnol.* **2017**, *43*, 34−40.

(7) Wishart, D. S.; Jewison, T.; Guo, A. C.; Wilson, M.; Knox, C.; Liu, Y.; Djoumbou, Y.; Mandal, R.; Aziat, F.; Dong, E.; Bouatra, S.; Sinelnikov, I.; Arndt, D.; Xia, J.; Liu, P.; Yallou, F.; Bjorndahl, T.; Perez-Pineiro, R.; Eisner, R.; Allen, F.; Neveu, V.; Greiner, R.; Scalbert, A. *Nucleic Acids Res.* **2012**, *41* (D1), D801−D807.

(8) Bingol, K.; Zhang, F.; Bruschweiler-Li, L.; Brüschweiler, R. *Anal. Chem.* **2012**, *84* (21), 9395−9401.
(9) Akiyama, K.; Chikayama, E.; Yuasa, H.; Shimada, Y.; Tohge, T.; Shinozaki, K.; Hirai, M. Y.; Sakurai, T.; Kikuchi, J.; Saito, K. *In Silico Biol.* **2008**, *8* (3−4), 339−45.
(10) Markley, J. L.; Ulrich, E. L.; Berman, H. M.; Henrick, K.; Nakamura, H.; Akutsu, H. *J. Biomol. NMR* **2008**, *40*, 153−155.
(11) Bingol, K.; Li, D.-W.; Bruschweiler-Li, L.; Cabrera, O. A.; Megraw, T.; Zhang, F.; Brüschweiler, R. *ACS Chem. Biol.* **2015**, *10* (2), 452−459.
(12) Zhang, F.; Brüschweiler, R. *Angew. Chem., Int. Ed.* **2007**, *46* (15), 2639−2642.
(13) Clendinen, C. S.; Lee-McMullen, B.; Williams, C. M.; Stupp, G. S.; Vandenborne, K.; Hahn, D. A.; Walter, G. A.; Edison, A. S. *Anal. Chem.* **2014**, *86* (18), 9242−9250.
(14) Clendinen, C. S.; Pasquel, C.; Ajredini, R.; Edison, A. S. *Anal. Chem.* **2015**, *87* (11), 5698−5706.
(15) Bhinderwala, F.; Lonergan, S.; Woods, J.; Zhou, C.; Fey, P. D.; Powers, R. *Anal. Chem.* **2018**, *90* (7), 4521−4528.
(16) Hattori, A.; Tsunoda, M.; Konuma, T.; Kobayashi, M.; Nagy, T.; Glushka, J.; Tayyari, F.; McSkimming, D.; Kannan, N.; Tojo, A.; Edison, A. S.; Ito, T. *Nature* **2017**, *545*, 500.
(17) Gorenstein, D. G. *Phosphorous-31 NMR: Principles and applications*; Academic Press: 2012.
(18) Gradwell, M. J.; Fan, T. W. M.; Lane, A. N. *Anal. Biochem.* **1998**, *263* (2), 139−149.
(19) Tolman, C. J.; Kanodia, S.; Roberts, M. F.; Daniels, L. *Biochim. Biophys. Acta, Mol. Cell Res.* **1986**, *886* (3), 345−352.
(20) Kühl, O. The Range of Chemical Shifts, Coupling Constants, and What Influences Each. In *Phosphorus-31 NMR Spectroscopy: A Concise Introduction for the Synthetic Organic and Organometallic Chemist*; Kühl, O., Ed.; Springer Berlin Heidelberg: Berlin, Heidelberg, 2008; pp 7−23, DOI: 10.1007/978-3-540-79118-8_2.
(21) Abi-Ghanem, J.; Heddi, B.; Foloppe, N.; Hartmann, B. *Nucleic Acids Res.* **2010**, *38* (3), e18−e18.
(22) Kellogg, G. W.; Schweitzer, B. I. *J. Biomol. NMR* **1993**, *3* (5), 577−595.
(23) Marino, J. P.; Schwalbe, H.; Anklin, C.; Bermel, W.; Crothers, D. M.; Griesinger, C. *J. Am. Chem. Soc.* **1994**, *116* (14), 6472−6473.
(24) Clendinen, C. S.; Lee-McMullen, B.; Williams, C. M.; Stupp, G. S.; Vandenborne, K.; Hahn, D. A.; Walter, G. A.; Edison, A. S. *Anal. Chem.* **2014**, *86* (18), 9242−9250.
(25) Edison, A. S.; Le Guennec, A.; Delaglio, F.; Kupce, E. *Methods Mol. Biol.* **2019**, *2037* (NMR-BasedMetabolomics), 69−95.
(26) Kluger, R.; Wasserstein, P.; Nakaoka, K. *J. Am. Chem. Soc.* **1975**, *97* (15), 4298−4303.
(27) Williams, G. D.; Mosher, T. J.; Smith, M. B. *Anal. Biochem.* **1993**, *214* (2), 458−467.
(28) Stein, A.; Crothers, D. M. *Biochemistry* **1976**, *15* (1), 160−168.
(29) Gorenstein, D. G.; Kar, D. *Biochem. Biophys. Res. Commun.* **1975**, *65* (3), 1073−1080.
(30) Bhinderwala, F.; Lonergan, S.; Woods, J.; Zhou, C.; Fey, P. D.; Powers, R. *Anal. Chem.* **2018**, *90* (7), 4521−4528.
(31) Tewari, Y. B.; Steckler, D. K.; Goldberg, R. N.; Gitomer, W. L. *J. Biol. Chem.* **1988**, *263* (8), 3670−5.
(32) Taqui Khan, M. M.; Srinivas Mohan, M. *J. Inorg. Nucl. Chem.* **1974**, *36* (3), 707−709.
(33) Worley, B.; Powers, R. *J. Magn. Reson.* **2015**, *261* (December 2015), 19−26.
(34) Webb, M. R.; Standring, D. N.; Knowles, J. R. *Biochemistry* **1977**, *16* (12), 2738−41.
(35) Cohn, M. *J. Biol. Chem.* **1949**, *180* (2), 771−781.
(36) Tredwell, G. D.; Bundy, J. G.; De Iorio, M.; Ebbels, T. M. D. *Metabolomics* **2016**, *12* (10), 152.
(37) Beneduci, A.; Chidichimo, G.; Dardo, G.; Pontoni, G. *Anal. Chim. Acta* **2011**, *685* (2), 186−195.
(38) Halouska, S.; Fenton, R. J.; Barletta, R. G.; Powers, R. *ACS Chem. Biol.* **2012**, *7* (1), 166−71.

https://dx.doi.org/10.1021/acs.analchem.0c00591
Anal. Chem. 2020, 92, 9536−9545